

Fully tunable coherence and control of acceptor qubits in Si

J. C. Abadillo-Uriel,^{1,2} Joe Salfi,² Xuedong Hu,^{2,3} Sven Rogge,² M. J. Calderón,¹ and Dimitrie Culcer⁴

¹*Instituto de Ciencia de Materiales de Madrid, ICMM-CSIC, Cantoblanco, E-28049 Madrid (Spain).*

²*School of Physics and Centre for Quantum Computation and Communication Technology, The University of New South Wales, Sydney 2052, Australia*

³*Department of Physics, University at Buffalo, SUNY, Buffalo, New York 14260-1500, USA*

⁴*School of Physics and Australian Research Council Centre of Excellence in Low-Energy Electronics Technologies, UNSW Node, The University of New South Wales, Sydney 2052, Australia*

(Dated: August 15, 2022)

Electrical control of quantum bits could pave the way for scalable quantum computation. An acceptor spin qubit in Si, based on spin-3/2 holes, can be controlled by electrical means using a gate electrode, which offers fast one- and two-qubit rotations and long coherence times at certain *sweet spots*. The relaxation time T_1 , while allowing $> 10^5$ operations, is the primary limiting factor. Here we show that, due to the interplay of the T_d symmetry of the acceptor in the Si lattice and the spin-3/2 characteristic of hole systems, an applied in-plane magnetic field strongly enhances the performance and coherence properties of the qubit. An appropriate choice of magnetic field orientation leads to a near-total suppression of spin relaxation as well as full tunability of two-qubit operations in a parameter regime in which dephasing due to charge fluctuations can be eliminated. Interestingly for spintronic applications, we find an extreme in-plane anisotropy such that the in-plane g -factor can vanish under certain circumstances.

Introduction. A scalable quantum computer architecture requires long qubit coherence times for its constituents [1, 2]. For spin qubits in semiconductors, the search for coherence has led to silicon [3–8], where hyperfine interaction with nuclear spins can be removed by isotopic enrichment [9, 10], piezoelectric interaction with phonons is entirely absent [11], and compatibility with Si microtechnology is of great help in nanofabrication [12].

Fast and high-fidelity control is another essential ingredient. In this context, electrical manipulation of spin qubits [13–15] is attracting considerable attention [16–20], as electric fields are significantly easier to apply and localize than magnetic fields, and use much less power [21]. However, coupling a spin to an electric field requires a strong spin-orbit interaction (SOI) in general [22–26], which typically makes the system sensitive to charge noise and phonons [27, 28]. Hence, the simultaneous improvement of electrical control and minimization of charge-noise induced decoherence are both key objectives in the search for scalable solid state quantum computers.

Over the past few years, a series of experimental and theoretical studies [25, 29–32] have shone a new light on the spins of acceptor-confined holes in Si, which possess multiple characteristics required by a scalable qubit: the finite spin-orbit coupling in the valence band [33–35] allows fast electrical control, and the Si substrate removes decoherence from nuclear magnetic noise [4, 8]. Furthermore, in a recent proposal [25] it has been shown that hybridization of light and heavy holes leads to sweet spots where decoherence due to charge noise could be suppressed. To date, experiments on confined holes have only scratched the surface of the vast potential of these systems for quantum coherent applications [36–45].

In this work we demonstrate a new control parameter that can tune the most important properties of an accep-

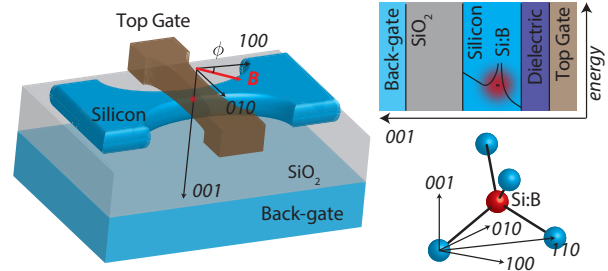


FIG. 1: (Color online) Sketch of the device geometry and layered heterostructure in the (001) direction. The orientation of the magnetic field within the plane is given by ϕ , the angle with respect to the (100) direction.

tor spin qubit, revealing a hitherto unexpected flexibility. Specifically, the T_d symmetry of an acceptor [46, 47] in Si gives rise to a strong interaction between the acceptor qubit and an electric field, making the qubit sensitive to the orientation of the in-plane magnetic field relative to the crystal axes. This gives us a powerful tool to tune the qubit couplings to the environment. At the sweet spots where the qubit is already insensitive to charge noise to first order, we find a decoherence free subspace (DFS), where the qubit is isolated from phonon and charge-noise-induced relaxation processes. Coupling between acceptor qubits can also be turned on and off at will with in-plane magnetic fields. The g -factor can be completely suppressed, useful for spintronic applications [45, 48–50]. The physical mechanism behind this strong tunability lies in the interplay between the qubit spin polarization induced by the T_d terms and the in-plane magnetic field.

Model. The Hamiltonian for a hole bound to an accep-

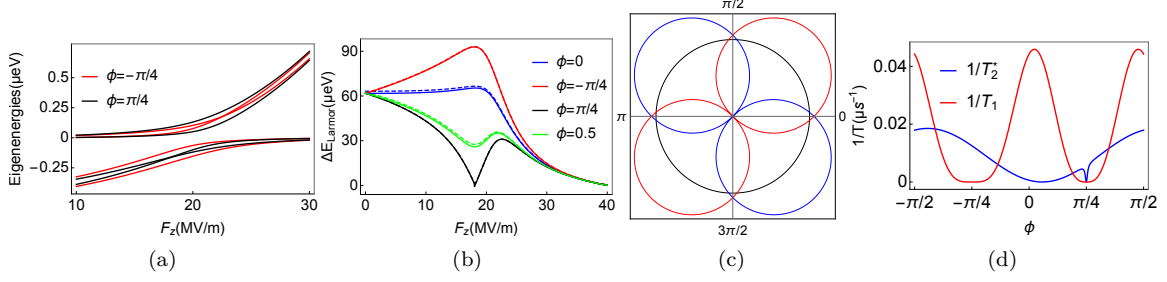


FIG. 2: (Color online) In all plots $B = 0.5$ T. (a) Eigenenergies of H_{eff} as a function of the vertical field for two particular cases $\phi = \pi/4$ (black lines) and $\phi = -\pi/4$ (red lines). (b) Larmor energy for different magnetic field orientations as a function of the vertical electric field. The Larmor energy at the fixed sweet spot ($F_z = 18.1$ MV/m) is enhanced for $\pi/2 < \phi < \pi$ and depressed for $0 < \phi < \pi/2$ with a minimum at $\phi = \pi/4$. At this point the two lowest levels cross. The dashed lines correspond to the numerical results. (c) g -factors as a function of the magnetic field orientation of the qubit states at $F_z = 0$ (black), $F_z^* = 18.1$ MV/m (blue) and the upper branch at $\tilde{F}_z = 22.5$ MV/m. (d) Inverse of the relaxation, see Eq. 6, and coherence times at F_z^* . $1/T_2^* = \Delta E_{\text{Larmor}}^2 \tau / 2\hbar^2$, with ΔE_{Larmor} given in Eq. 5, is obtained assuming $\delta E_{\parallel} = 3\text{kV/m}$ in the x direction and a switching time $\tau = 10^{-6}$ s.

tor in a Si/SiO₂ nanostructure, see Fig. 1, is

$$H = H_{KL} + H_{BP} + H_c + H_{\text{inter}} + H_F + H_B + H_{T_d} \quad (1)$$

which contains the valence band Kohn-Luttinger Hamiltonian [51] H_{KL} including cubic symmetry terms, the strain Bir-Pikus term [46, 47] H_{BP} , the acceptor Coulomb potential H_c , the (001) Si/SiO₂ interface H_{inter} , the interaction with electric H_F and magnetic field $H_B = g_1\mu_B\mathbf{B}\cdot\mathbf{J} + g_2\mu_B\mathbf{B}\cdot\mathbf{J}^3$, including both the linear and cubic contributions. Tensile strain is needed for the qubit to have LH character [25, 52], which is critical for a strong Zeeman interaction with an *in-plane* magnetic field [53].

The local T_d symmetry of the acceptor gives rise to a linear coupling of the total effective spin \mathbf{J} with the electric field \mathbf{F} of the form [54] $H_{T_d} = \frac{p}{\sqrt{3}} (\{J_y, J_z\}F_x + \{J_x, J_z\}F_y + \{J_x, J_y\}F_z)$ where p is an effective dipole moment that can be calculated [55] by $p = e \int_0^a f^*(r)r f(r)$ with a the lattice constant of the host material, and $f(r)$ the radial envelope function. For a boron acceptor in Si $p = 0.26$ Debye. This value is larger in deep acceptors, with a smaller Bohr radius [55]. H_{T_d} is also linearly proportional to the strength of the electric field. We neglect the other allowed T_d symmetric terms as their coupling constants are much smaller [47].

Importantly, H_{T_d} reduces the cubic symmetry to T_d , giving a previously unnoticed prominence to the orientation of the in-plane magnetic field. This symmetry reduction gives rise to an electric field dependent anisotropy that affects each state differently. Such an anisotropy is normally negligible below the ionization field [56]. However, the SiO₂ interface increases the ionization field, yielding a dramatic anisotropy of the g -factors.

Effective Hamiltonian. We use the effective mass approach described in Ref. [32]. Expanding over the ground state manifold and using the $\{3/2, 1/2, -1/2, -3/2\}$ basis [25, 52], the effective Hamiltonian of an acceptor qubit

for an arbitrary in-plane orientation ϕ of \mathbf{B} is

$$H_{\text{eff}} = \begin{pmatrix} 0 & \frac{\sqrt{3}}{2}\varepsilon_Z e^{-i\phi} & -ipF_z & 0 \\ \frac{\sqrt{3}}{2}\varepsilon_Z e^{i\phi} & \Delta_{HL} & \varepsilon_Z e^{-i\phi} & -ipF_z \\ ipF_z & \varepsilon_Z e^{i\phi} & \Delta_{HL} & \frac{\sqrt{3}}{2}\varepsilon_Z e^{-i\phi} \\ 0 & ipF_z & \frac{\sqrt{3}}{2}\varepsilon_Z e^{i\phi} & 0 \end{pmatrix} \quad (2)$$

$\phi = 0$ for \mathbf{B} along the x -direction, given by one of the main crystal axes. The cubic g -factor g_2 [55] is not explicitly shown in Eq. 2, but is included in the numerical calculations. The Zeeman term is $\varepsilon_Z = g_1\mu_B B$. The HH energy is set to zero for $F_z = 0$. At zero fields, the strain conditions are such that $\Delta_{HL} < 0$ and the ground state is of LH character. As shown in Fig. 2(a), the magnitude of Δ_{HL} decreases as F_z increases. The bound hole wave-function is pushed towards the interface eventually leading to a LH-HH anticrossing and a HH ground state.

In the absence of a magnetic field, we can diagonalize Hamiltonian (2) and obtain two (Kramers) degenerate branches, with eigenenergies $E_l = \frac{1}{2}(\Delta_{HL} - \sqrt{\Delta_{HL}^2 + 4p^2 F_z^2})$ and $E_u = \frac{1}{2}(\Delta_{HL} + \sqrt{\Delta_{HL}^2 + 4p^2 F_z^2})$, respectively, for the lower and upper branches. As long as $\Delta_{HL} < 0$, the lower branch would be LH-like, with $a_L = E_l / \sqrt{E_l^2 + p^2 F_z^2}$ and $a_H = pF_z / \sqrt{E_l^2 + p^2 F_z^2}$ the LH and HH probability amplitudes of both states. These two states in the lower-energy branch encode our qubit.

Qubit operating point Hamiltonian. The qubit is operated in a finite in-plane magnetic field to optimize its coherence and maneuverability. Rotating H_{eff} to the qubit basis (see Supplemental Material [57]), we obtain

$$H_{\text{op}} = \begin{pmatrix} E_l - \frac{1}{2}\varepsilon_{Zl} & 0 & Z_1 & Z_2 \\ 0 & E_l + \frac{1}{2}\varepsilon_{Zl} & Z_2 & Z_1 \\ Z_1 & -Z_2 & E_u - \frac{1}{2}\varepsilon_{Zu} & 0 \\ -Z_2 & Z_1 & 0 & E_u + \frac{1}{2}\varepsilon_{Zu} \end{pmatrix} \quad (3)$$

where ε_{Zl} and ε_{Zu} are the Larmor energy of the lower (qubit) and upper branches respectively, while Z_1 and Z_2 are Zeeman coupling induced HH-LH mixings, both directly proportional to ε_{Zo} [57]. Explicitly,

$$\begin{aligned}\varepsilon_{Zl} &= 2\varepsilon_Z \sqrt{3a_L^2 a_H^2 + a_L^4 + 2\sqrt{3}a_L^3 a_H \sin(2\phi)} \\ \varepsilon_{Zu} &= 2\varepsilon_Z \sqrt{3a_L^2 a_H^2 + a_H^4 - 2\sqrt{3}a_L^3 a_H \sin(2\phi)} \\ \varepsilon_{Zo} &= 2\varepsilon_Z \sqrt{a_H^2 a_L^2 + (a_L^2 - a_H^2)(3/4 - \sqrt{3}a_H a_L \sin(2\phi))}.\end{aligned}\quad (4)$$

Due to the strong SOI arising from H_{T_d} , these couplings depend on both the magnetic field in-plane orientation ϕ and on F_z through a_H and a_L . The different LH and HH weights in an eigenstate imply a complex combination of J_z eigenstates $\{3/2, 1/2, -1/2, -3/2\}$. The system eigenstates thus have different angular momentum projections L_z and S_z such that an electric field not only modifies the orbital angular momentum but also the spin polarization (defined in [57]). Therefore, changing a_L and a_H strongly affects the spin polarization of the qubit.

One important consequence of the complex interplay between electric and magnetic fields is the existence of sweet spots where the qubit splitting is insensitive to charge noise, with the positions of the sweet spots dependent on ϕ , the in-plane magnetic field orientation. There are two solutions to $d\varepsilon_{Zl}/dF_z = 0$. One is a *fixed* (independent of ϕ) sweet spot at $F_z^* = -\frac{\sqrt{3}\Delta_{HL}}{2p}$ corresponding to $a_L = -\sqrt{3}/2$. Here the LH and HH contributions are such that the Larmor frequency can increase or decrease as a function of ϕ , see Fig. 2(b). The other one, the *mobile* (dependent on ϕ) sweet spot at \tilde{F}_z , is determined by $a_H + \sqrt{3}a_L \sin 2\phi = 0$. Positive solutions of \tilde{F}_z require $0 \leq \phi \leq \pi/2$ or $\pi \leq \phi \leq 3\pi/2$. For $\phi = 0$ or $\pi/2$ this *mobile* sweet spot is at $\tilde{F}_z = 0$. For intermediate values of ϕ , it swings from $\tilde{F}_z = 0$ to a maximum $\tilde{F}_z = \frac{\sqrt{3}\Delta_{HL}}{2p}$ at $\phi = \pi/4$ and back to $\tilde{F}_z = 0$. For $\pi/2 \leq \phi \leq \pi$, \tilde{F}_z is negative, a regime which is not relevant for the manipulation of a qubit in the considered geometry.

At these two sweet spots the spin polarization is spin-orbit induced and independent of the magnetic field. At F_z^* the spin of the qubit is polarized in the $-\pi/4 + n\pi$ direction while, at the maximum value of \tilde{F}_z , the spin of the upper branch is polarized in the $\pi/4 + n\pi$ direction. This fixed spin polarization has several consequences. When a magnetic field is applied perpendicularly to the induced spin polarization the effective g -factor goes to zero, see Fig. 2(c), and these states cannot sense the magnetic field. On the other hand, the effective g -factor is maximized when the in-plane magnetic field is parallel to the spin polarization. In this case $[H_{\text{inter}} + H_{T_d}, H_B] = 0$, such that the qubit and upper subspaces are fully decoupled, with $\varepsilon_{Zo} = 0$. Since the qubit states are manipulated via their coupling to the upper branch, the decoupling here means the qubit is fully isolated from the environment: Neither an experimenter nor external noises

can affect it, making the qubit decoherence free. Compared to the conventional DFSs, where decoherence is suppressed via the symmetries of the encoded states, the DFS here is achieved by actively controlling the strength of its interaction with the environment.

Dephasing due to charge noise. The crucial role played by SOI in the qubit implies that the main threat of decoherence stems from electrical noises, particularly background charge fluctuations induced dephasing [58, 59]. It is already known that this qubit is insensitive up to first order to in-plane electric field fluctuations and, at the sweet spots, also to vertical electric field fluctuations [25]. Among the residue effects of the charge noise, the strongest second-order contribution comes from in-plane noise as it couples to the Rashba coupling α , which is maximized near the sweet spots [25].

We consider in-plane charge noise caused by charging and discharging of nearby interface defects [60]. The electric field fluctuation at the acceptor is $(\delta E_x, \delta E_y, 0) = \delta E_{\parallel}(\cos \theta_{\parallel}, \sin \theta_{\parallel}, 0)$. The perturbation Hamiltonian includes both the Rashba SOI (with coupling α , see [57]) and H_{T_d} , and couples the qubit and upper branch states.

For large vertical fields, such as at the sweet spots, $\alpha \gg p$ and, after taking a Schrieffer-Wolff (SW) transformation [61, 62] to account for the impact of the noise in the qubit sub-manifold, we obtain the expression for the fluctuation in the Larmor energy due to charge noise

$$\Delta E_{\text{Larmor}} = \alpha^2 \frac{\delta E_{\parallel}^2}{(E_l - E_u)^2} [\varepsilon_{Zl} + \varepsilon_{Zu} \cos(2(\theta + \theta_{\parallel}))]. \quad (5)$$

Here $\theta = (\theta_u - \theta_l)/2$ is a phase that depends on the applied electric and magnetic fields (for more details, including definitions of θ_l and θ_u , see [57]). ε_{Zl} , ε_{Zu} and θ all depend on ϕ allowing the minimization of ΔE_{Larmor} . Particularly, when ε_{Zl} is smaller than ε_{Zu} , it can be set to zero. This implies a minimal condition for the applied vertical field $\Delta_{HL} + 2\sqrt{3}pF_z \sin(2\phi) > 0$. The effect of this charge noise on $1/T_2^*$ as a function of ϕ is illustrated in Fig. 2(d) at the fixed sweet spot.

Phonon induced relaxation. Spin-relaxation occurs via the deformation potential interaction [11]. At the sweet spots the relaxation rate is given by

$$\frac{1}{T_1} = \frac{(\hbar\omega(\phi))^3}{20\hbar^4\pi\rho} C_d \left(\frac{\varepsilon_{Zo}(\phi)}{\Delta} \right)^2 \quad (6)$$

where $C_d = 4.9 \times 10^{-20} (\text{eV})^2 (\text{s/m})^5$ is a combination of Si deformation potentials [25]. The dependence on ϕ of $\hbar\omega$ and ε_{Zo}/Δ is different for each sweet spot. At the fixed sweet spot F_z^* and $\phi = 0$, T_1 is estimated to be $\sim 20\mu\text{s}$ for 0.5T but near $\phi = \pi/4 + n\pi$ the qubit frequency $\hbar\omega(\phi)$ is suppressed, significantly increasing T_1 as shown in Fig. 2(d). However, at this point other spin relaxation mechanisms may become relevant. In contrast, $\hbar\omega(\phi)$ cannot be suppressed at the mobile sweet spot \tilde{F}_z .

Full suppression of $1/T_1$ can also be achieved in the DFS. In this case the applied magnetic field points in the

spin-polarization direction, induced by the T_d symmetry at the sweet spots. When this happens the qubit and upper branches are decoupled ($\varepsilon_{Z_o} = 0$), eliminating this relaxation mechanism as shown in Fig. 2(d).

Electric dipole spin resonance. As indicated in [57], an in-plane electric field couples the LH and HH states via the Rashba SOI. When both in-plane electric and magnetic fields are present, the effective two-level Hamiltonian for a single qubit can be simplified to $H_{\text{qubit}} = \hbar\omega\sigma_z + DE_{\parallel}\sigma_x$. The transverse coupling $DE_{\parallel}\sigma_x$ allows driving of the qubit via an AC electric field. For an incoming in-plane electric field $\mathbf{E}_{\parallel} = E_{\parallel}(\cos\theta_{\parallel}, \sin\theta_{\parallel})$ the EDSR coupling D is

$$D = \frac{\varepsilon_{Z_o}(\phi)}{E_u - E_l} (\alpha \cos(\theta_o(\phi) - \theta_{\parallel}) + p \sin(\theta_o(\phi) - \theta_{\parallel})). \quad (7)$$

For the fixed sweet spot, $\theta_o = \pi/4$, independent of the magnetic field orientation ϕ , and $\varepsilon_{Z_o} \propto \sqrt{1 + \sin(2\phi)}$. Hence, EDSR is switched off for $\phi = 3\pi/4 + n\pi$ as expected because this corresponds to the isolation of the qubit levels. At the mobile sweet spot, $\varepsilon_{Z_o} \propto \cos(2\phi)$ and hence EDSR is switched off for $\phi = \pi/4 + n\pi$.

Two-qubit coupling. The magnetic field in-plane orientation can also be used to completely switch off two-qubit coupling mediated by the electric dipolar interaction between acceptor pairs [63–65] $H_{dd} = (\mathbf{v}^a \cdot \mathbf{v}^b R^2 - 3(\mathbf{v}^a \cdot \mathbf{R})(\mathbf{v}^b \cdot \mathbf{R})) / 4\pi\epsilon R^5$. Here \mathbf{v}^i is the total charge dipole of qubit i , and typical optimal distances between acceptors are of the order of tens of nm, which also allows us to neglect tunneling between the two acceptors. In the two-qubit subspace, H_{dd} can be written as an Ising type interaction $H_{dd} = J_{dd}(\sigma_+^a + \sigma_-^a)(\sigma_+^b + \sigma_-^b)$. The coupling strength J_{dd} is a function of the relative position between the acceptors a and b , which we define as $\mathbf{R} = R \cos(\theta_E)\hat{x} + R \sin(\theta_E)\hat{y}$. Here we have neglected the difference in the acceptor depths, which can be made much smaller than the in-plane distance. Then:

$$J_{dd} = \frac{\alpha^a \alpha^b \varepsilon_{Z_o}^a \varepsilon_{Z_o}^b}{8\pi\epsilon R^3 \Delta^a \Delta^b} G(F_z^a, F_z^b, \phi, \theta_E), \quad (8)$$

where $G(F_z^a, F_z^b, \phi, \theta_E)$ is a function that depends on the operating point of each qubit, and is plotted in Fig. 3(a). Notice that J_{dd} not only depends on the applied fields F_z^i , but also on ϕ through both ε_{Z_o} and G .

As shown in Eq. (8) and Fig. 3, J_{dd} can vanish for particular parameter choices. Specifically, each qubit should always be operated at a sweet spot, so that there are three different combinations for two qubits: (i) both qubits are at their fixed sweet spots; (ii) one qubit is at the fixed while the other is at the mobile sweet spot; (iii) both qubits are at their mobile sweet spots.

In case (i) the two-qubit interaction is switched off for $\phi = 3\pi/4 + n\pi$, since in the DFS the qubits are robust against any interaction. For this case $G(F_z^{*a}, F_z^{*b}, \phi, \theta_E) = 1$, hence the coupling is independent of θ_E , the relative orientation of the acceptors. In

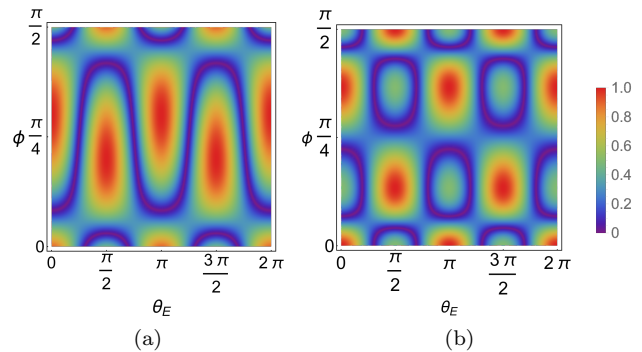


FIG. 3: (Color online) Normalized $G(F_z^a, F_z^b, \phi, \theta_E)$, see Eq. 8. (a) Case (ii): $F_z^a = F_z^{*a}$ and $F_z^b = F_z^b$. (b) Case (iii): $F_z^a = \tilde{F}_z^a$ and $F_z^b = \tilde{F}_z^b$.

(ii) J_{dd} can be switched off for $\phi = \pi/4 + n\pi/2$ and there is an explicit dependence on θ_E , shown in Fig. 3(a): for each θ_E there is at least one ϕ that can be used to switch off J_{dd} . In case (iii), the interaction is switched off for $\phi = \pi/4 + n\pi$. However, $G(\tilde{F}_z^a, \tilde{F}_z^b, \phi, \theta_E)$ cannot be switched off for all values of θ_E , as shown in Fig. 3(b).

We thus conclude that the orientation of \mathbf{B} can first be chosen such that the coupling in case (ii) is zero, whereupon the vertical electric field can be used to switch to case (i) allowing the possibility of turning on and off the two-qubit coupling by simply changing the top gate for each qubit. This mechanism paves the way for entanglement and two-qubit operations in this system.

Conclusions. For an acceptor in Si near a Si/SiO₂ interface, the strong interaction with the interface electric field due to terms with T_d symmetry gives rise to a complex in-plane magnetic field orientation dependence of the coherence times, and single- and two-qubit gates. This makes it possible to create a decoherence-free subspace where both dephasing and relaxation processes are suppressed, increase or decrease the EDSR coupling, and fully tune the electric-field mediated two-qubit coupling. We expect our work to stimulate state-of-the-art experiments on acceptor qubits, and pave the way towards fast, coherent and scalable quantum computation with confined hole systems.

JCAU and MJC acknowledge funding from Ministerio de Economía, Industria y Competitividad (Spain) via Grants No FIS2012-33521 and FIS2015-64654-P and from CSIC (Spain) via grant No 201660I031. JCAU thanks the support from grants BES-2013-065888 and EEBB-I-16-11046. DC and SR are supported by the Australian Research Council Centres of Excellence FLEET (CE170100039) and CQC2T (CE110001027), respectively. XH thanks support by US ARO through grant W911NF1210609, and Gordon Godfrey Fellowship from UNSW School of Physics. JS acknowledges financial support from an ARC DECRA fellowship (DE160101490).

SUPPLEMENTARY INFORMATION

KOHN-LUTTINGER AND BIR-PIKUS HAMILTONIANS

The Kohn-Luttinger Hamiltonian for the valence band of semiconductors, including the Coulomb impurity, is $H_{\text{KL}} =$

$$\begin{pmatrix} P+Q & L & M & 0 & \frac{i}{\sqrt{2}}L & -i\sqrt{2}M \\ L^* & P-Q & 0 & M & -i\sqrt{2}Q & i\sqrt{\frac{3}{2}}L \\ M^* & 0 & P-Q & -L & -i\sqrt{\frac{3}{2}}L^* & -i\sqrt{2}Q \\ 0 & M^* & -L^* & P+Q & -i\sqrt{2}M^* & -\frac{i}{\sqrt{2}}L^* \\ -i\sqrt{2}L^* & i\sqrt{2}Q & i\sqrt{\frac{3}{2}}L & i\sqrt{2}M & P+\Delta_{\text{SO}} & 0 \\ i\sqrt{2}M^* & -i\sqrt{\frac{3}{2}}L^* & i\sqrt{2}Q & i\sqrt{2}L & 0 & P+\Delta_{\text{SO}} \end{pmatrix} \quad (\text{S1})$$

We can define the effective Rydberg unit as $Ry^* = e^4 m_0 / 2 \hbar^2 \epsilon_s^2 \gamma_1$ and the effective Bohr radius as $a^* = \hbar^2 \epsilon_s \gamma_1 / e^2 m_0$. In these units the differential operators in Eq. (S1) are

$$\begin{aligned} P &= -k^2 + \frac{2}{r} \\ Q &= -\frac{\gamma_2}{\gamma_1}(k_x^2 + k_y^2 - 2k_z^2) \\ L &= i2\sqrt{3}\frac{\gamma_3}{\gamma_1}(k_x - ik_y)k_z \\ M &= -\sqrt{3}\frac{\gamma_2}{\gamma_1}(k_x^2 - k_y^2) + i2\sqrt{3}\frac{\gamma_3}{\gamma_1}k_x k_y, \end{aligned} \quad (\text{S2})$$

with m_0 the free electron mass, ϵ_s the semiconductor static dielectric constant, and γ_1 , γ_2 and γ_3 material dependent Luttinger parameters. The interaction with strain is given by the Bir-Pikus Hamiltonian:

$$\begin{aligned} H_{\text{BP}} &= a\epsilon_{\mathbb{1}} \\ &+ b \left((J_x^2 - \frac{5}{4}\mathbb{1})\epsilon_{xx} + (J_y^2 - \frac{5}{4}\mathbb{1})\epsilon_{yy} + (J_z^2 - \frac{5}{4}\mathbb{1})\epsilon_{zz} \right) \\ &+ d/\sqrt{3} (\{J_x, J_y\}\epsilon_{xy} + \{J_y, J_z\}\epsilon_{yz} + \{J_x, J_z\}\epsilon_{xz}) \end{aligned} \quad (\text{S3})$$

The parameters a, b and d are the deformation potentials of the host material, ϵ_{ij} are the deformation tensor components.

EFFECTIVE 4 × 4 HAMILTONIAN

The results of the diagonalization of the total Hamiltonian are mapped onto an effective Hamiltonian for the four lowest states. For any magnetic field orientation ϕ the Hamiltonian in the $|m_J\rangle$ basis is:

$$H_{\text{eff}} = \begin{pmatrix} 0 & \frac{\sqrt{3}}{2}\epsilon_Z e^{-i\phi} & -ipF_z & 0 \\ \frac{\sqrt{3}}{2}\epsilon_Z e^{i\phi} & \Delta_{HL} & \epsilon_Z e^{-i\phi} & -ipF_z \\ ipF_z & \epsilon_Z e^{i\phi} & \Delta_{HL} & \frac{\sqrt{3}}{2}\epsilon_Z e^{-i\phi} \\ 0 & ipF_z & \frac{\sqrt{3}}{2}\epsilon_Z e^{i\phi} & 0 \end{pmatrix} \quad (\text{S4})$$

The presence of the T_d terms makes the magnetic field orientation a physically relevant parameter.

To define the qubit, first, we consider the Hamiltonian when no magnetic field is applied:

$$H_{op}(\epsilon_Z = 0) = \begin{pmatrix} 0 & 0 & -ipF_z & 0 \\ 0 & \Delta_{HL} & 0 & -ipF_z \\ ipF_z & 0 & \Delta_{HL} & 0 \\ 0 & ipF_z & 0 & 0 \end{pmatrix} \quad (\text{S5})$$

Defining $E_l = \frac{1}{2}(\Delta_{HL} - \sqrt{\Delta_{HL}^2 + 4p^2 F_z^2})$, $E_u = \frac{1}{2}(\Delta_{HL} + \sqrt{\Delta_{HL}^2 + 4p^2 F_z^2})$, $a_L = E_l / \sqrt{E_l^2 + p^2 F_z^2}$ and $a_H = pF_z / \sqrt{E_l^2 + p^2 F_z^2}$, the previous Hamiltonian is diagonalized being E_l and E_u the energies of the lower and upper branches respectively. The unitary transformation that makes the diagonalization to the new basis $\{l-, l+, u-, u+\}$ is:

$$U_0 = \begin{pmatrix} -ia_H & 0 & 0 & a_L \\ 0 & a_L & ia_H & 0 \\ a_L & 0 & 0 & -ia_H \\ 0 & ia_H & a_L & 0 \end{pmatrix} \quad (\text{S6})$$

Applying this unitary transformation to the original Hamiltonian we get:

$$\hat{H}_{op} = \begin{pmatrix} E_l & \frac{1}{2}\lambda_{Zl}^* & \frac{1}{2}\lambda_{Zo}^* & 0 \\ \frac{1}{2}\lambda_{Zl} & E_l & 0 & \frac{1}{2}\lambda_{Zo} \\ \frac{1}{2}\lambda_{Zo} & 0 & E_u & \frac{1}{2}\lambda_{Zu}^* \\ 0 & \frac{1}{2}\lambda_{Zo}^* & \frac{1}{2}\lambda_{Zu} & E_u \end{pmatrix} \quad (\text{S7})$$

In this basis the Zeeman interaction is the only off-diagonal term, with

$$\begin{aligned} \lambda_{Zl} &= 2\epsilon_Z (a_L^2 e^{-i\phi} - i\sqrt{3}a_L a_H e^{i\phi}) \\ \lambda_{Zu} &= 2\epsilon_Z (-a_H^2 e^{i\phi} + i\sqrt{3}a_L a_H e^{-i\phi}) \\ \lambda_{Zo} &= 2\epsilon_Z (-ia_H a_L e^{-i\phi} + \sqrt{3}(a_L^2 - a_H^2))e^{i\phi}/2 \end{aligned} \quad (\text{S8})$$

For a general magnetic field orientation the off-diagonal couplings are orientation dependent. We can now do the last transformation to define the qubit. Let the unperturbed Hamiltonian be:

$$U_0^\dagger H_{op,0} U_0 = \begin{pmatrix} E_l & \frac{1}{2}\lambda_{Zl}^* & 0 & 0 \\ \frac{1}{2}\lambda_{Zl} & E_l & 0 & 0 \\ 0 & 0 & E_u & \frac{1}{2}\lambda_{Zu}^* \\ 0 & 0 & \frac{1}{2}\lambda_{Zu} & E_u \end{pmatrix} \quad (\text{S9})$$

This Hamiltonian is diagonalized by U_{Z0} to give the eigenenergies $E_{\pm} = E_l \pm \frac{1}{2}|\lambda_{Zl}|$ and $E_{u\pm} = E_u \pm \frac{1}{2}|\lambda_{Zu}|$. Writing $\lambda_{Zl} = \epsilon_{Zl} \exp(i\theta_l)$, $\lambda_{Zu} = \epsilon_{Zu} \exp(i\theta_u)$, and $\lambda_{Zo} = \epsilon_{Zo} \exp(i\theta_o)$,

$$\begin{aligned}
\theta_l &= \arctan(a_L^2 \cos(\phi) + \sqrt{3}a_L a_H \sin(\phi), -a_L^2 \sin(\phi) - \sqrt{3}a_L a_H \cos(\phi)) \\
\theta_u &= \arctan(-a_H^2 \cos(\phi) + \sqrt{3}a_L a_H \sin(\phi), -a_H^2 \sin(\phi) + \sqrt{3}a_L a_H \cos(\phi)) \\
\theta_o &= \arctan(-a_L a_H \sin(\phi) + \sqrt{3}/2(a_L^2 - a_H^2) \cos(\phi), -a_L a_H \cos(\phi) + \sqrt{3}/2(a_L^2 - a_H^2) \sin(\phi))
\end{aligned} \tag{S10}$$

$$\begin{aligned}
\varepsilon_{Zl} &= 2\varepsilon_Z \sqrt{3a_L^2 a_H^2 + a_L^4 + 2\sqrt{3}a_L^3 a_H \sin(2\phi)} \\
\varepsilon_{Zu} &= 2\varepsilon_Z \sqrt{3a_L^2 a_H^2 + a_H^4 - 2\sqrt{3}a_H^3 a_L \sin(2\phi)} \\
\varepsilon_{Zo} &= 2\varepsilon_Z \sqrt{3(a_L^2 - a_H^2)/4 + a_H^2 a_L^2 + \sqrt{3}a_H a_L (a_H^2 - a_L^2) \sin(2\phi)}
\end{aligned} \tag{S11}$$

The unitary transformation that diagonalizes the previous Hamiltonian is then:

$$U_{Z0} = 2^{-\frac{1}{2}} \begin{pmatrix} e^{-i\theta_l/2} & e^{-i\theta_l/2} & 0 & 0 \\ -e^{i\theta_l/2} & e^{i\theta_l/2} & 0 & 0 \\ 0 & 0 & e^{-i\theta_u/2} & e^{-i\theta_u/2} \\ 0 & 0 & -e^{i\theta_u/2} & e^{i\theta_u/2} \end{pmatrix} \tag{S12}$$

The Hamiltonian in this basis is:

$$H_{qubit} = \begin{pmatrix} E_l - \frac{1}{2}\varepsilon_{Zl} & 0 & Z_1 & Z_2 \\ 0 & E_l + \frac{1}{2}\varepsilon_{Zl} & Z_2 & Z_1 \\ Z_1 & -Z_2 & E_u - \frac{1}{2}\varepsilon_{Zu} & 0 \\ -Z_2 & Z_1 & 0 & E_u - \frac{1}{2}\varepsilon_{Zu} \end{pmatrix} \tag{S13}$$

where

$$\begin{aligned}
Z_1 &= \frac{1}{2}\varepsilon_{Zo} \cos(\theta_l/2 - \theta_u/2 - \theta_o) \\
Z_2 &= \frac{i}{2}\varepsilon_{Zo} \sin(\theta_l/2 - \theta_u/2 - \theta_o)
\end{aligned} \tag{S14}$$

Here Z_i are the Zeeman interactions between the lower and upper branches. Note that Z_1 is a real number while Z_2 is a purely imaginary number.

EFFECTIVE RASHBA INTERACTION

The qubit operations are performed by applying in-plane oscillating electric fields. The presence of the interface breaks the inversion symmetry of the envelope wavefunctions allowing the mixing of states with different behavior under the parity operator. This lack of inversion symmetry allows the action of an in-plane linear Stark effect $H_E = e(E_x x + E_y y) = eE_{\parallel}(\cos\theta_{\parallel} + \sin\theta_{\parallel})$. The effect of this interaction of the acceptor hole is calculated considering several excited states and mapped onto the effective 4×4 Hamiltonian in the $|m_J\rangle$ basis:

$$H_E = E_{\parallel} \begin{pmatrix} 0 & \alpha e^{i\theta_{\parallel}} & 0 & 0 \\ \alpha e^{-i\theta_{\parallel}} & 0 & 0 & 0 \\ 0 & 0 & 0 & -\alpha e^{i\theta_{\parallel}} \\ 0 & 0 & -\alpha e^{-i\theta_{\parallel}} & 0 \end{pmatrix} \tag{S15}$$

Where α is an effective Rashba coupling, associated to the lack of inversion symmetry, and related to the applied vertical electric field and the distance to the interface. This effective Rashba Hamiltonian, rotated into the qubit basis becomes

$$\hat{H}_E = \begin{pmatrix} 0 & 0 & E_{1R} & E_{2R} \\ 0 & 0 & E_{2R} & E_{1R} \\ -E_{1R} & E_{2R} & 0 & 0 \\ E_{2R} & -E_{1R} & 0 & 0 \end{pmatrix} \tag{S16}$$

Being

$$\begin{aligned}
E_{1R} &= i\alpha E_{\parallel} \sin(\theta_{\parallel} + \theta) \\
E_{2R} &= -\alpha E_{\parallel} \cos(\theta_{\parallel} + \theta)
\end{aligned} \tag{S17}$$

Where $\theta = \theta_u/2 - \theta_l/2$.

SWEET SPOTS

The value of the qubit Larmor frequency is given, to first order, by ε_{Zl} . Its value depends explicitly on both the electric field and magnetic field magnitudes, but also depends on the magnetic field orientation. We can look for sweet spots by simply finding the solutions to $d\varepsilon_{Zl}/dF = 0$:

$$\frac{d\varepsilon_{Zl}}{dF_z} = \varepsilon_Z \frac{(-3 + 4a_L^2)(a_H + \sqrt{3}a_L \sin(2\phi))a'_L(F_z)}{a_H \sqrt{3 - 2a_L^2 + 2\sqrt{3}a_L a_H \sin(2\phi)}} = 0 \tag{S18}$$

One of the solutions corresponds to the fixed sweet spot $a_L = -\sqrt{3}/2$ ($a_H = 1/2$). Considering that $a'_L \propto a_H$, the other solution is equivalent to solve $a_H + \sqrt{3}a_L \sin(2\phi) = 0$. Considering positive electric fields $a_H \geq 0$ and $a_L \leq 0$, meaning that for $0 \leq \phi \leq \pi/2$ and $\pi \leq \phi \leq 3\pi/2$ there is a ϕ dependent sweet spot solution.

Particularly, at $\phi = \pi/4 + n\pi$ this corresponds to $a_H = \sqrt{3}/2$ and $a_L = -1/2$ while for a magnetic field aligned with the main axes of the crystal, this sweet spot corresponds to the value $F_z = 0$.

Also, when $\phi = \pi/4 + n\pi$ the value of the Larmor frequency at the fixed sweet spot is zero. For electric

fields lesser than F_z^* the spin polarization, given by θ_l , is the opposite to the spin polarization after F_z^* , meaning that an effective g -factor flip occurs in this particular case.

CHARGE NOISE

Lets consider an in-plane charge noise perturbation $(\delta E_x, \delta E_y, 0) = \delta E_{\parallel}(\cos(\theta_{\parallel}), \sin(\theta_{\parallel}))$. Its Hamiltonian

$$H_{noise} = \delta E_{\parallel} \begin{pmatrix} 0 & \alpha e^{i\theta_{\parallel}} + ipe^{-i\theta_{\parallel}} & 0 & 0 \\ \alpha e^{-i\theta_{\parallel}} - ipe^{i\theta_{\parallel}} & 0 & 0 & 0 \\ 0 & 0 & 0 & -\alpha e^{i\theta_{\parallel}} - ipe^{-i\theta_{\parallel}} \\ 0 & 0 & -\alpha e^{-i\theta_{\parallel}} + ipe^{i\theta_{\parallel}} & 0 \end{pmatrix} \quad (S19)$$

Which, rotated into the qubit basis is:

$$\hat{H}_{noise} = \begin{pmatrix} 0 & 0 & E_1 & E_2 \\ 0 & 0 & E_2 & E_1 \\ -E_1 & E_2 & 0 & 0 \\ E_2 & -E_1 & 0 & 0 \end{pmatrix} \quad (S20)$$

where

$$\begin{aligned} E_1 &= i\delta E_{\parallel}(p \cos(\theta_{\parallel} - \theta) + \alpha \sin(\theta_{\parallel} + \theta)) \\ E_2 &= -\delta E_{\parallel}(p \sin(\theta_{\parallel} - \theta) + \alpha \cos(\theta_{\parallel} + \theta)) \end{aligned} \quad (S21)$$

Note that E_1 is a purely imaginary quantity while E_2 is a real number.

in the $|m_J\rangle$ basis is:

We can now consider the effective 2×2 Hamiltonian using a SW transformation. The first order is identically zero but the second order adds corrections to both the diagonal and off-diagonal terms. Let the interaction term be $H' = \hat{H}_{noise} + \hat{H}_Z$, where the latter term are the off-diagonal Zeeman interactions. The second order correction is

$$\Delta H_{m,m'}^{(2)} = \frac{1}{2} \sum_l H'_{m,l} H'_{l,m'} \left(\frac{1}{E_m - E_l} + \frac{1}{E'_m - E_l} \right) \quad (S22)$$

For the dephasing term we get:

$$\begin{aligned} \Delta H_{--}^{(2)} - \Delta H_{++}^{(2)} &= (E_1 + Z_1)(E_1^* + Z_1^*) \left(\frac{1}{E_l - E_u - \varepsilon_{Zl}/2 + \varepsilon_{Zu}/2} - \frac{1}{E_l - E_u + \varepsilon_{Zl}/2 - \varepsilon_{Zu}/2} \right) \\ &\quad + (E_2 + Z_2)(E_2^* + Z_2^*) \left(\frac{1}{E_l - E_u - \varepsilon_{Zl}/2 + \varepsilon_{Zu}/2} - \frac{1}{E_l - E_u + \varepsilon_{Zl}/2 - \varepsilon_{Zu}/2} \right) \end{aligned} \quad (S23)$$

As for a given i the terms Z_i and E_i are one purely imaginary and the other purely real, we have:

$$\begin{aligned} (E_i + Z_i)(E_i^* + Z_i^*) &= |E_i|^2 + |Z_i|^2 + (E_i Z_i^* + E_i^* Z_i) \\ &= |E_i|^2 + |Z_i|^2 \end{aligned} \quad (S24)$$

The terms linear in the in-plane electric fields are identi-

cally zero. Moreover, the terms involving $|Z_i|^2$ are static, being irrelevant for this analysis. Expanding to first order the fraction terms, the expression for dephasing is:

$$\Delta E_{Larmor}^{noise} = |E_1|^2 \frac{\varepsilon_{Zl} - \varepsilon_{Zu}}{(E_l - E_u)^2} + |E_2|^2 \frac{\varepsilon_{Zu} + \varepsilon_{Zl}}{(E_l - E_u)^2} \quad (S25)$$

Which, after substituting expressions becomes:

$$\Delta E_{Larmor}^{noise} = \frac{\delta E_{\parallel}^2}{(E_l - E_u)^2} \left[(\alpha \sin(\theta + \theta_{\parallel}) + p \cos(\theta - \theta_{\parallel}))^2 (\varepsilon_{Zl} - \varepsilon_{Zu}) + (\alpha \cos(\theta + \theta_{\parallel}) - p \sin(\theta - \theta_{\parallel}))^2 (\varepsilon_{Zu} + \varepsilon_{Zl}) \right] \quad (S26)$$

In the limit of large α , which is valid for example at the fixed sweet spot, we can further simplify this expression:

$$\Delta E_{\text{Larmor}}^{\text{noise}} = \alpha^2 \frac{\delta E_{\parallel}^2}{(E_l - E_u)^2} \left[\varepsilon_{Zl}(\phi) + \varepsilon_{Zu}(\phi) \cos(2(\theta(\phi) + \theta_{\parallel})) \right] \quad (\text{S27})$$

This expression can be set to zero by carefully choosing ϕ for several combinations, but not always. For those cases in which this is not possible it is still possible to minimize as a function of ϕ .

DECOHERENCE FREE SUBSPACE (DFS)

As the qubit interacts with the HH states through the Zeeman interaction, we can see this subspace as a leakage submanifold. The interaction terms between the qubit states and the leakage states are then given by the off-diagonal Zeeman terms in the qubit Hamiltonian. A decoherence and relaxation free subspace would be a subspace in which the Zeeman interaction is purely diagonal in the qubit basis, or equivalently $[H_{T_d} + H_{\text{interface}}, H_B] = 0$. In this subspace, all the interactions would be suppressed to first order. To find this subspace we use the following elements that form part of a bigger basis of the space of spin 3/2:

$$\begin{aligned} e_1 &= \frac{\mathbb{1}}{2} \\ e_2 &= 1/6(2J_z^2 - J_x^2 - J_y^2) \\ e_3 &= 1/\sqrt{5}J_x \\ e_4 &= 1/\sqrt{5}J_y \\ e_5 &= 1/\sqrt{12}\{J_x, J_y\} \\ e_6 &= 1/\sqrt{12}\{J_y, J_z\} \\ e_7 &= 1/\sqrt{12}\{J_z, J_x\} \end{aligned} \quad (\text{S28})$$

In this basis the elements of the effective Hamiltonian are

$$\begin{aligned} H_{\text{inter}} &= \Delta_{HL}(e_1 - e_2) \\ H_{T_d} &= 2pF_z e_5 \\ H_B &= \sqrt{5}(B_x e_3 + B_y e_4) \end{aligned} \quad (\text{S29})$$

The commutators are then

$$\begin{aligned} [H_{\text{inter}}, H_B] &= i2\sqrt{3}\Delta_{HL}(B_y e_7 - B_x e_6) \\ [H_{T_d}, H_B] &= -4ipF_z(B_x e_7 - B_y e_6) \end{aligned} \quad (\text{S30})$$

The total commutator is

$$\begin{aligned} [H_{\text{inter}} + H_{T_d}, H_B] &= e_7(-4ipF_z B_x + i2\sqrt{3}\Delta_{HL}B_y) \\ &+ e_6(4ipF_z B_y - i2\sqrt{3}\Delta_{HL}B_x) \end{aligned} \quad (\text{S31})$$

As e_7 and e_6 are different elements of the basis, $[H_{\text{inter}} + H_{T_d}, H_B] = 0$ is equivalent to solve the follow-

ing system

$$\begin{aligned} \Delta_{HL}B_y - \frac{2pF_z}{\sqrt{3}}B_x &= 0 \\ \Delta_{HL}B_x - \frac{2pF_z}{\sqrt{3}}B_y &= 0 \end{aligned} \quad (\text{S32})$$

The system has non-trivial solutions if and only if $B_x = \pm B_y$ which corresponds to the orientations $\pm\pi/4 + n\pi$. These are the most symmetric directions as the main axes of the crystal remain indistinguishable.

Case $B_x = -B_y$, the solution requires $\Delta_{HL} = -\frac{2pF_z}{\sqrt{3}}$ which corresponds to the fixed sweet spot. The case $B_x = B_y$ requires $\Delta_{HL} = \frac{2pF_z}{\sqrt{3}}$ corresponding to the mobile sweet spot. In these two cases the Zeeman interaction can be diagonalized simultaneously with the interface and T_d symmetry terms, so the qubit becomes isolated from the upper branch.

It is also interesting to express the different contributions in terms of the spherical tensors J_+ and J_-

$$\begin{aligned} H_{T_d} + H_{\text{inter}} &= -\frac{3}{4}\mathbb{1} - \frac{i}{8}(\Delta_{HL} + 2pF_z/\sqrt{3})(J_+ + iJ_-)^2 \\ &+ \frac{i}{8}(\Delta_{HL} - 2pF_z/\sqrt{3})(J_+ - iJ_-)^2 \\ H_B &= \frac{1+i}{4}(B_x - B_y)(J_+ - iJ_-) \\ &+ \frac{1-i}{4}(B_x + B_y)(J_+ + iJ_-) \end{aligned} \quad (\text{S33})$$

From here it can be seen how for the sweet spots, and for particular values of the magnetic fields, the non-magnetic and the magnetic terms share eigenvectors.

SPIN POLARIZATION INDUCED BY THE SPIN-ORBIT INTERACTION

The qubit states in the $|m_J\rangle$ basis are:

$$|l\pm\rangle = a_L|\pm 1/2\rangle \mp ia_H|\mp 3/2\rangle \quad (\text{S34})$$

Transforming the m_J basis into the $|l_z, s_z\rangle$ basis using the Clebsch-Gordan coefficients

$$|l\pm\rangle = \frac{a_L}{\sqrt{3}}(|\pm 1, \mp 1/2\rangle + \sqrt{2}|0, \pm 1/2\rangle) \mp ia_H|\mp 1, \mp 1/2\rangle \quad (\text{S35})$$

To get the spin polarization of this states we can compute the matrix of expected values for the in-plane spin operators $\langle l'|\sigma_i|l\rangle$:

$$\langle l'|\sigma_x|l\rangle = \frac{a_L}{3} \begin{pmatrix} 0 & a_L + i\sqrt{3}a_H \\ a_L - i\sqrt{3}a_H & 0 \end{pmatrix} \quad (\text{S36})$$

$$\langle l'|\sigma_y|l\rangle = \frac{a_L}{3} \begin{pmatrix} 0 & ia_L + \sqrt{3}a_H \\ -ia_L + \sqrt{3}a_H & 0 \end{pmatrix} \quad (\text{S37})$$

At the fixed sweet spot $a_L = -\sqrt{3}/2$ and $a_H = 1/2$, making $\langle l'|\sigma_x|l\rangle = -\langle l'|\sigma_y|l\rangle$, and at the same time the expected value at the direction $\phi = -\pi/4$ becomes saturated to the maximum possible value of spin projection equals to 1/2 which is equivalent to a spin polarization in the $\phi = -\pi/4 \pm \pi$ direction. The other interesting possibility is $a_L = -1/2$ and $a_H = \sqrt{3}/2$ which corresponds to the mobile sweet spot in the particular case $\phi = \pi/4$. In this case the upper states have the composition $a_L = -\sqrt{3}/2$ and $a_H = 1/2$ so $\langle u'|\sigma_x|u\rangle = \langle u'|\sigma_y|u\rangle$ indicating a spin polarization of the upper branch in the $\phi = \pi/4 \pm \pi$.

At the sweet spots the spin polarization, related to θ_l and θ_u , of the branch with bigger LH contribution is fixed. Particularly at the fixed sweet spot, the qubit is spin polarized in the $-\pi/4 + n\pi$ in-plane direction while at the mobile sweet spot the polarization is fixed at $\pi/4 + n\pi$ for the upper branch. When the magnetic field points in the same direction as the spin polarization, the eigenstates of the spin-orbit terms coincide with those of the magnetic field leading to a DFS, isolating the upper and lower branches. In contrast, when the magnetic field points perpendicularly to the spin polarization fixed by the spin-orbit terms, the result is that the magnetic field contribution is suppressed leading to a zero effective g -factor, see Fig. 2(a).

In the supplemental movie (see ancillary files) the spin polarization of the lowest state is shown as a function of a_H and the magnetic field orientation. It can be seen how at the sweet spot ($a_H = 1/2$) this polarization is fixed.

ELECTRIC DIPOLE SPIN RESONANCE

We consider here the effects of an oscillating in-plane electric field produced by the gates. The Hamiltonian is analogous to Eq.(S20) but with an electric field given by (E_x, E_y) . We can perform the same SW transformation in Eq.(S22) to obtain the off-diagonal term

$$H_{-+}^{(2)} = \frac{2\varepsilon_{Zu}\text{Re}(-Z_1Z_2)}{(E_l - E_u)^2} + \frac{2\varepsilon_{Zu}\text{Re}(-E_1E_2)}{(E_l - E_u)^2} + \frac{2\text{Re}(E_2Z_1 - E_1Z_2)}{(E_l - E_u)} \quad (\text{S38})$$

The first two terms are identically zero because Z_1 and E_2 are real numbers while Z_2 and E_1 are purely imaginary. The last terms are linear in the electric field so this is the EDSR term. Substituting the expressions we get:

$$H_{-+}^{(2)} = \frac{1}{2} \frac{\varepsilon_{Zo}(\phi)}{E_l - E_u} \delta E_{\parallel} (\alpha \cos(\theta_o(\phi) - \theta_{\parallel}) + p \sin(\theta_o(\phi) - \theta_{\parallel})) \quad (\text{S39})$$

This expression is valid for both sweet spots.

PHONON-INDUCED SPIN RELAXATION

At low temperatures the expression for the relaxation times of the acceptor qubit is:

$$\frac{1}{T_1} = \frac{(\hbar\omega)^3}{20\hbar^4\pi\rho} \left[\sum_i |\langle -|D_{ii}|+\rangle|^2 \left(\frac{2}{v_i^5} + \frac{4}{3v_i^5} \right) + \sum_{i \neq j} |\langle -|D_{ij}|+\rangle|^2 \left(\frac{2}{3v_i^5} + \frac{1}{v_i^5} \right) \right] \quad (\text{S40})$$

Going to second order in the SW transformation we get:

$$\langle -|D_{ij}|+\rangle = \frac{1}{E_l - E_u} (\hat{H}'_{-,u-} \hat{H}'_{u-,+} + \hat{H}'_{-,u+} \hat{H}'_{u+,+}) \quad (\text{S41})$$

Where $\hat{H}' = \hat{H}'_Z + \hat{H}'_{ph}$. The elements of the Hamiltonian \hat{H}'_{ph} are:

$$D_{ii} = b'(J_i^2 - \frac{5}{4}) \\ D_{ij} = 2d'/\sqrt{3}\{J_i, J_j\} \quad i \neq j \quad (\text{S42})$$

The values of $|\langle -|D_{ij}|+\rangle|^2$ at the fixed sweet spot are independent on the angle ϕ except for the intrinsic dependence of ε_{Zo} . These values are

$$|\langle -|D_{xx}|+\rangle|^2 = |\langle -|D_{yy}|+\rangle|^2 = 3b^2\varepsilon_{Zo}^2/64\Delta^2 \\ |\langle -|D_{zz}|+\rangle|^2 = 3b^2\varepsilon_{Zo}^2/16\Delta^2 \\ |\langle -|D_{xy}|+\rangle|^2 = d^2\varepsilon_{Zo}^2/16\Delta^2 \\ |\langle -|D_{xz}|+\rangle|^2 = |\langle -|D_{yz}|+\rangle|^2 = d^2\varepsilon_{Zo}^2/8\Delta^2 \quad (\text{S43})$$

In the case of the mobile sweet spot the values of $|\langle -|D_{ij}|+\rangle|^2$ are

$$|\langle -|D_{xx}|+\rangle|^2 = |\langle -|D_{yy}|+\rangle|^2 = 3b^2\varepsilon_{Zo}^2/64\Delta^2 \\ |\langle -|D_{zz}|+\rangle|^2 = 3b^2\varepsilon_{Zo}^2/16\Delta^2 \\ |\langle -|D_{xy}|+\rangle|^2 = d^2\varepsilon_{Zo}^2/16\Delta^2 \\ |\langle -|D_{xz}|+\rangle|^2 = d^2\varepsilon_{Zo}^2 \cos^2 \theta_o / 4\Delta^2 \\ |\langle -|D_{yz}|+\rangle|^2 = d^2\varepsilon_{Zo}^2 \sin^2 \theta_o / 4\Delta^2 \quad (\text{S44})$$

Collecting terms, the new dependence on the phase θ_o cancels out so we arrive to the same formula except for different definitions of ε_{Zo} and the energy difference $\Delta = E_l - E_u$.

The general formula for phonon-induced relaxation at the sweet spots is then

$$\frac{1}{T_1} = \frac{(\hbar\omega(\phi))^3}{20\hbar^4\pi\rho} \left(\frac{\varepsilon_{Z_o}(\phi)}{E_l - E_u} \right)^2 \left[\frac{3b'}{32} \left(\frac{2}{v_l^5} + \frac{4}{3v_t^5} \right) + \frac{5d'}{48} \left(\frac{2}{3v_l^5} + \frac{1}{v_t^5} \right) \right] \quad (\text{S45})$$

TWO QUBIT COUPLING

Assuming two acceptors separated by a distance \mathbf{R} . Due to the spin-orbit interaction and the electric dipole moment of each acceptor a spin-dependent dipolar interaction is expected between the two acceptors. Let the subspace of the two qubits be $\{|l^{-a}, l^{-b}\rangle, |l^{-a}, l^{+b}\rangle, |l^{+a}, l^{-b}\rangle, |l^{+a}, l^{+b}\rangle\}$. The total Hamiltonian is $H^\Sigma = H_{op}^a + H_{op}^b + V^{12}$, where H_{op} are the single acceptor Hamiltonians and V^{12} is the Hamiltonian of the electrostatic interaction given by $V^{12}(\mathbf{r}_1 - \mathbf{r}_2) = e^2/4\pi\epsilon|\mathbf{r}_1 - \mathbf{r}_2|$.

Here we assume that each qubit may have different en-

ergies and applied fields. The single qubit Hamiltonians are:

$$\langle m|H_{op}^i|m'\rangle = \begin{pmatrix} -\frac{\varepsilon_l^i}{2} & 0 & Z_1^i & iZ_2^i \\ 0 & \frac{\varepsilon_l^i}{2} & iZ_2^i & Z_1^i \\ Z_1^i & -iZ_2^i & \Delta^i - \frac{\varepsilon_l^i}{2} & 0 \\ -iZ_2^i & Z_1^i & 0 & \frac{\varepsilon_l^i}{2} + \Delta^i \end{pmatrix} \quad (\text{S46})$$

Where the superindex i indicates acceptor a or b.

When the two acceptors are far enough we can use the multi-pole expansion for the Coulomb interaction:

$$\langle mn|V^{12}|m'n'\rangle = \frac{R^2 \langle m|\mathbf{er}'_1|m'\rangle \cdot \langle n|\mathbf{er}'_2|n'\rangle - 3(\langle m|\mathbf{er}'_1|m'\rangle \cdot \mathbf{R})(\langle n|\mathbf{er}'_2|n'\rangle \cdot \mathbf{R})}{4\pi\epsilon R^5} \quad (\text{S47})$$

Being $\mathbf{r}'_i = \mathbf{r}_i - \mathbf{R}_i$ the hole coordinate relative to the ion, and assuming an arbitrary relative position in the xy plane $\mathbf{R} = R \cos(\theta_E)\hat{x} + R \sin(\theta_E)\hat{y}$, so

$$\langle mn|V^{12}|m'n'\rangle = \frac{(1 - 3 \cos^2 \theta_E) \langle m|ex'_1|m'\rangle \cdot \langle n|ex'_2|n'\rangle + (1 - 3 \sin^2 \theta_E) \langle m|ey'_1|m'\rangle \cdot \langle n|ey'_2|n'\rangle + \langle m|ez'_1|m'\rangle \cdot \langle n|ez'_2|n'\rangle}{4\pi\epsilon R^3} \quad (\text{S48})$$

The dipole matrix elements relevant for the Coulomb interaction are:

$$\langle m|e(x', y')^i|m'\rangle = \begin{pmatrix} 0 & 0 & iq_{1x,y}^i & q_{2x,y}^i \\ 0 & 0 & q_{2x,y}^i & iq_{1x,y}^i \\ -iq_{1x,y}^i & q_{2x,y}^i & 0 & 0 \\ q_{2x,y}^i & -iq_{1x,y}^i & 0 & 0 \end{pmatrix} \quad (\text{S49})$$

where $q_{1x}^i = \alpha^i \sin \theta^i$, $q_{2x}^i = -\alpha^i \cos \theta^i$, $q_{1y}^i = \alpha^i \cos \theta^i$, and $q_{2y}^i = \alpha^i \sin \theta^i$ (assuming the approximation $\alpha \gg p$ valid for both qubits).

We can project the interactions into the 4×4 subspace using a SW transformation. The second order correction is given in equation (S22). Working out $H^{(2)}$ to zeroth order in ε_i gives a spin-independent shift:

$$H^{(2)} = -I \left[\frac{((q_1^a)^2 + (q_2^a)^2) ((q_1^b)^2 + (q_2^b)^2)}{\Delta^a + \Delta^b} + \frac{(Z_1^a)^2 + (Z_2^b)^2}{\Delta^a} + \frac{(Z_1^b)^2 + (Z_2^a)^2}{\Delta^b} \right] \quad (\text{S50})$$

The third-order correction is

$$H_{mm'}^{(3)} = -\frac{1}{2} \sum_{l,m''} \left[\frac{H'_{ml} H'_{lm''} H'_{m''m}}{(E_{m'} - E_l)(E_{m''} - E_l)} + \frac{H'_{mm''} H'_{m''l} H'_{lm'}}{(E_m - E_l)(E_{m''} - E_l)} \right] \\ + \frac{1}{2} \sum_{l,l'} H'_{ml'} H'_{ll'} H'_{l'm'} \left[\frac{1}{(E_m - E_l)(E_m - E_{l'})} + \frac{1}{(E_{m'} - E_l)(E_{m'} - E_{l'})} \right] \quad (\text{S51})$$

The result of the third order correction to zeroth order in ε_i is

$$H^{(3)} = J_{dd} \begin{pmatrix} 0 & 0 & 0 & 1 \\ 0 & 0 & 1 & 0 \\ 0 & 1 & 0 & 0 \\ 1 & 0 & 0 & 0 \end{pmatrix} \quad (\text{S52})$$

where

$$J_{dd} = \frac{4(q_2^a Z_1^a + q_1^a Z_2^a)(q_2^b Z_1^b + q_1^b Z_2^b)}{\Delta^a \Delta^b} \quad (\text{S53})$$

Which is an Ising type spin-spin interaction

$$H^{(3)} = J_{dd}(\sigma_{a+} + \sigma_{a-})(\sigma_{b+} + \sigma_{b-}).$$

After adding all the contributions and substituting, the value of J_{dd} is:

$$J_{dd} = \frac{\alpha^a \alpha^b \varepsilon_{Z_o}^a \varepsilon_{Z_o}^b (\sin \theta_o^a \sin \theta_o^b (1 - 3 \sin^2 \theta_E) + \cos \theta_o^a \cos \theta_o^b (1 - 3 \cos^2 \theta_E))}{4\pi \epsilon R^3 (E_l^a - E_u^a)(E_l^b - E_u^b)} \quad (\text{S54})$$

This expression can be substituted for each case

Case (i): We get:

$$J_{dd} = \frac{3}{2} \varepsilon_Z^2 (1 + \sin(2\phi)) \frac{\alpha^a \alpha^b}{8\pi \epsilon R^3 (E_l^a - E_u^a)(E_l^b - E_u^b)} \quad (\text{S55})$$

Case (ii): Omitting the complex dependence in the dynamic sweet spot of θ_o on ϕ :

$$J_{dd} = 3\varepsilon_Z^2 \sqrt{1 + \sin(2\phi)} \frac{\alpha^a \alpha^b |\cos(2\phi)|^2 (3 \cos(3\phi - \theta_o^a) - \cos(\phi + \theta_o^a) - 3 \cos(2\theta_E)(\cos(\phi - \theta_o^a) - 3 \cos(3\phi + \theta_o^a)))}{16\pi \epsilon R^3 (E_l^a - E_u^a)(E_l^b - E_u^b) \sqrt{7 + 4 \cos 4\phi - 3 \cos 8\phi}} \quad (\text{S56})$$

Case (iii):

$$J_{dd} = 3\varepsilon_Z^2 \frac{\alpha^a \alpha^b \cos^2(2\phi) [(1 - 3 \cos^2 \theta_E) \cos \theta_o^a \cos \theta_o^b + (1 - 3 \sin^2 \theta_E)] \sin \theta_o^a \sin \theta_o^b}{8\pi \epsilon R^3 (E_l^a - E_u^a)(E_l^b - E_u^b) (3 \cos(4\phi) - 5)} \quad (\text{S57})$$

-
- [1] M. A. Nielsen and I. L. Chuang, *Quantum Computation and Quantum Information: 10th Anniversary Edition* (Cambridge University Press, New York, NY, USA, 2011), 10th ed., ISBN 1107002176, 9781107002173.
- [2] A. G. Fowler, M. Mariantoni, J. M. Martinis, and A. N. Cleland, *Phys. Rev. A* **86**, 032324 (2012).
- [3] A. M. Tyryshkin, J. J. L. Morton, S. C. Benjamin, A. Ardavan, G. A. D. Briggs, J. W. Ager, and S. A. Lyon, *Journal of Physics: Condensed Matter* **18**, S783 (2006).
- [4] J. T. Muhonen, J. P. Dehollain, A. Laucht, F. E. Hudson, R. Kalra, T. Sekiguchi, K. M. Itoh, D. N. Jamieson, J. C. McCallum, A. S. Dzurak, et al., *Nat Nano* **9**, 986 (2014).
- [5] C. Tahan and R. Joynt, *Phys. Rev. B* **71**, 075315 (2005).
- [6] L. Wang, K. Shen, B. Y. Sun, and M. W. Wu, *Phys. Rev. B* **81**, 235326 (2010).
- [7] M. Raith, P. Stano, and J. Fabian, *Phys. Rev. B* **83**, 195318 (2011).
- [8] M. Veldhorst, J. C. C. Hwang, C. H. Yang, A. W. Leenstra, B. de Ronde, J. P. Dehollain, J. T. Muhonen, F. E. Hudson, K. M. Itoh, A. Morello, et al., *Nat Nano* **9**, 981 (2014).

-
- [9] E. Abe, K. M. Itoh, J. Isoya, and S. Yamasaki, *Phys. Rev. B* **70**, 033204 (2004).
- [10] K. M. Itoh and H. Watanabe, *MRS Communications* **4**, 143157 (2014).
- [11] H. Ehrenreich and A. W. Overhauser, *Phys. Rev.* **104**, 331 (1956).
- [12] R. Maurand, X. Jehl, D. Kotekar-Patil, A. Corna, H. Bohuslavskiy, R. Laviéville, L. Hutin, S. Barraud, M. Vinet, M. Sanquer, et al., *Nature Communications* **7**, 13575 EP (2016).
- [13] D. Loss and D. P. DiVincenzo, *Phys. Rev. A* **57**, 120 (1998).
- [14] B. E. Kane, *Nature* **393**, 133 (1998).
- [15] J. R. Petta, A. C. Johnson, J. M. Taylor, E. A. Laird, A. Yacoby, M. D. Lukin, C. M. Marcus, M. P. Hanson, and A. C. Gossard, *Science* **309**, 2180 (2005).
- [16] D. V. Bulaev and D. Loss, *Phys. Rev. Lett.* **98**, 097202 (2007).
- [17] K. C. Nowack, F. H. L. Koppens, Y. V. Nazarov, and L. M. K. Vandersypen, *Science* **318**, 1430 (2007).
- [18] J. Medford, J. Beil, J. M. Taylor, E. I. Rashba, H. Lu, A. C. Gossard, and C. M. Marcus, *Phys. Rev. Lett.* **111**, 050501 (2013).
- [19] C. Schirm, M. Matt, F. Pauly, J. C. Cuevas, P. Nielaba,

- and E. Scheer, *Nat Nano* **8**, 645 (2013).
- [20] J. Romhányi, G. Burkard, and A. Pályi, *Phys. Rev. B* **92**, 054422 (2015).
- [21] J. J. L. Morton, D. R. McCamey, M. A. Eriksson, and S. A. Lyon, *Nature* **479**, 345 (2011).
- [22] P. Szumniak, S. Bednarek, B. Partoens, and F. M. Peeters, *Phys. Rev. Lett.* **109**, 107201 (2012).
- [23] A. Pályi, P. R. Struck, M. Rudner, K. Flensberg, and G. Burkard, *Phys. Rev. Lett.* **108**, 206811 (2012).
- [24] M. Friesen, C. Tahan, R. Joynt, and M. A. Eriksson, *Phys. Rev. Lett.* **92**, 037901 (2004).
- [25] J. Salfi, J. A. Mol, D. Culcer, and S. Rogge, *Phys. Rev. Lett.* **116**, 246801 (2016).
- [26] J. Salfi, M. Tong, S. Rogge, and D. Culcer, *Nanotechnology* **27**, 244001 (2016).
- [27] A. Bermeister, D. Keith, and D. Culcer, *Applied Physics Letters* **105**, 192102 (2014).
- [28] R. Ruskov and C. Tahan, *Phys. Rev. B* **88**, 064308 (2013).
- [29] J. Van der Heijden, J. Salfi, J. A. Mol, J. Verduijn, G. C. Tettamanzi, A. R. Hamilton, N. Collaert, and S. Rogge, *Nano Letters* **14**, 1492 (2014).
- [30] J. van der Heijden, T. Kobayashi, M. House, J. Salfi, S. Barraud, R. Lavieville, M. Simmons, and S. Rogge, arXiv:1703.03538 [cond-mat.mes-hall] (2017).
- [31] J. A. Mol, J. Salfi, R. Rahman, Y. Hsueh, J. A. Miwa, G. Klimeck, M. Y. Simmons, and S. Rogge, *Applied Physics Letters* **106**, 203110 (2015).
- [32] J. C. Abadillo-Uriel and M. J. Calderón, *Nanotechnology* **27**, 024003 (2016).
- [33] R. Winkler, *Phys. Rev. B* **70**, 125301 (2004).
- [34] D. Culcer, C. Lechner, and R. Winkler, *Phys. Rev. Lett.* **97**, 106601 (2006).
- [35] R. Winkler, D. Culcer, S. J. Papadakis, B. Habib, and M. Shayegan, *Semiconductor Science and Technology* **23**, 114017 (2008).
- [36] G. Katsaros, P. Spathis, M. Stoffel, F. Fournel, M. Mongillo, V. Bouchiat, F. Lefloch, A. Rastelli, O. G. Schmidt, and S. De Franceschi, *Nat Nano* **5**, 458 (2010).
- [37] H. Watzinger, C. Kloeffel, L. Vukusic, M. D. Rossell, V. Sessi, J. Kuckucka, R. Kirchschrager, E. Lausecker, A. Truhlar, M. Glaser, et al., *Nano Letters* **16**, 6879 (2016).
- [38] A. V. Nenashev, A. V. Dvurechenskii, and A. F. Zinovieva, *Phys. Rev. B* **67**, 205301 (2003).
- [39] H. Malissa, W. Jantsch, M. Muhlberger, F. Schaffler, Z. Wilamowski, M. Draxler, and P. Bauer, *Applied Physics Letters* **85**, 1739 (2004).
- [40] N. Ares, V. N. Golovach, G. Katsaros, M. Stoffel, F. Fournel, L. I. Glazman, O. G. Schmidt, and S. De Franceschi, *Phys. Rev. Lett.* **110**, 046602 (2013).
- [41] A. Srinivasan, K. L. Hudson, D. Miserev, L. A. Yeoh, O. Klochan, K. Muraki, Y. Hirayama, O. P. Sushkov, and A. R. Hamilton, *Phys. Rev. B* **94**, 041406 (2016).
- [42] S. J. Prado, C. Trallero-Giner, A. M. Alcalde, V. López-Richard, and G. E. Marques, *Phys. Rev. B* **69**, 201310 (2004).
- [43] M. Kugler, T. Andlauer, T. Korn, A. Wagner, S. Fehringer, R. Schulz, M. Kubová, C. Gerl, D. Schuh, W. Wegscheider, et al., *Phys. Rev. B* **80**, 035325 (2009).
- [44] T. Andlauer and P. Vogl, *Phys. Rev. B* **79**, 045307 (2009).
- [45] A. J. Bennett, M. A. Pooley, Y. Cao, N. Sköld, I. Farrer, D. A. Ritchie, and A. J. Shields, *Nature Communications* **4**, 1522 (2013).
- [46] G. Bir, E. Butikov, and G. Pikus, *Journal of Physics and Chemistry of Solids* **24**, 1467 (1963).
- [47] G. Bir, E. Butikov, and G. Pikus, *Journal of Physics and Chemistry of Solids* **24**, 1475 (1963).
- [48] A. Oiwa, T. Fujita, H. Kiyama, G. Allison, A. Ludwig, A. D. Wieck, and S. Tarucha, *Journal of the Physical Society of Japan* **86**, 011008 (2017).
- [49] G. Salis, Y. Kato, K. Ensslin, D. C. Driscoll, A. C. Gosard, and D. D. Awschalom, *Nature* **414**, 619 (2001).
- [50] A. Bogan, S. A. Studenikin, M. Korkusinski, G. C. Aers, L. Gaudreau, P. Zawadzki, A. S. Sachrajda, L. A. Tracy, J. L. Reno, and T. W. Hargett, *Phys. Rev. Lett.* **118**, 167701 (2017).
- [51] J. M. Luttinger and W. Kohn, *Phys. Rev.* **97**, 869 (1955).
- [52] J. C. Abadillo-Uriel and M. J. Calderón, *New Journal of Physics* **19**, 043027 (2017).
- [53] Such an interaction is not only important for direct control of the qubit, but also essential if coupling to a superconductor resonator is sought [23, 63, 66–68].
- [54] Note that these terms are absent in spin-1/2 electron systems.
- [55] A. Köpf and K. Lassmann, *Phys. Rev. Lett.* **69**, 1580 (1992).
- [56] G. D. J. Smit, S. Rogge, J. Caro, and T. M. Klapwijk, *Phys. Rev. B* **70**, 035206 (2004).
- [57] Supplemental Material.
- [58] X. Hu and S. Das Sarma, *Phys. Rev. Lett.* **96**, 100501 (2006).
- [59] D. Culcer, X. Hu, and S. Das Sarma, *Applied Physics Letters* **95**, 073102 (2009).
- [60] D. Culcer and N. M. Zimmerman, *Applied Physics Letters* **102**, 232108 (2013).
- [61] J. R. Schrieffer and P. A. Wolff, *Phys. Rev.* **149**, 491 (1966).
- [62] R. Winkler, *Spin-orbit coupling effects in two-dimensional electron and hole systems*, Springer tracts in modern physics (Springer, Berlin, 2003).
- [63] M. Trif, V. N. Golovach, and D. Loss, *Phys. Rev. B* **77**, 045434 (2008).
- [64] V. N. Golovach, M. Borhani, and D. Loss, *Phys. Rev. B* **74**, 165319 (2006).
- [65] C. Flindt, A. S. Sørensen, and K. Flensberg, *Phys. Rev. Lett.* **97**, 240501 (2006).
- [66] C. Kloeffel, M. Trif, P. Stano, and D. Loss, *Phys. Rev. B* **88**, 241405 (2013).
- [67] X. Hu, Y. X. Liu, and F. Nori, *Phys. Rev. B* **86**, 035314 (2012).
- [68] L. Childress, A. S. Sørensen, and M. D. Lukin, *Phys. Rev. A* **69**, 042302 (2004).